AIAA JOURNAL
Vol. 45, No. 2, February 2007

Experimental Determination of the Dynamic Behavior of a Multifunctional Power Structure

C. W. Schwingshackl*
Imperial College London, London, SW7 2AZ England, United Kingdom
G. S. Aglietti†
University of Southampton, Southampton, SO17 1BJ England, United Kingdom
and
P. R. Cunningham‡
Smiths Aerospace Mechanical Systems-Aerostructures, Hamble-le Rice, SO31 4NF England, United Kingdom

DOI: 10.2514/1.23894

A main aim of spacecraft design is cost reduction that can either be achieved by reducing the cost of the spacecraft or by lowering the cost to launch. One proposed technology to reduce the mass and therefore lower the launch costs is the multifunctional power structure concept that incorporates the secondary spacecraft power supply into the load carrying structure. Here a short introduction of the dynamic analysis and optimization of such a structure is presented. The manufacture and testing of a multifunctional power panel is discussed in detail and its dynamic response is compared to a conventional honeycomb panel. The multifunctional design successfully combined the structural and power storage functions. It provided a similar dynamic response to conventional spacecraft structures and improved the energy density.

Nomenclature

$\mathrm{Ene}_{\mathrm{MFS}}$	=	energy stored in multifunctional structure
f	=	frequency
$G_{C_{xz,yz}}$	=	shear modulus of the core in xz and yz directions
m_{inert}	=	mass of the inert honeycomb panel
m_{MFS}	=	mass of the multifunctional structure
Γ	=	frequency-density ratio
ρ	=	material density

I. Introduction

A MAIN aim of spacecraft design is cost reduction while maintaining or expanding the mission objectives. This can be achieved either by reducing the cost of the spacecraft (design and manufacture) or by lowering the cost to launch. The mass plays a central role in this attempt as parametric cost models by the U.S. Air Force show that satellite cost is directly proportional to satellite mass [1]. To significantly reduce the costs of future missions it is necessary to lower the flight mass by an order of magnitude when compared to current spacecraft technologies [2,3].

In contrast to mass, volume, and cost reduction the technical expectations of these new classes of spacecraft are predicted to rise. To provide the necessary extended capabilities at a lower mass and volume, the implementation of recent advances in technology such as ultralight deployable systems [4] and nanotechnology [5] is required. A further approach to achieve this goal is the multifunctional structure (MFS) design, which merges the load carrying capabilities of traditional spacecraft structures with other stand alone functions. The main task of the structure is to support in an appropriate configuration the spacecraft equipment during launch and operation. The spacecraft structures, and, in particular, the enclosures of the different subsystems, currently also provide radiation shielding for the sensitive components and the thermal management for heat generating components (i.e., electronics). Hence they can be considered already partially multifunctional, and an expansion of their multifunctionality is an obvious next step in the development. This can be achieved by integrating other elements into the spacecraft structure.

In a previous study of a multifunctional power structure approach [6] the authors have introduced 10 possible MFS designs (see Fig. 1) based on the structural bicells developed by Boundless Corp. as disclosed in the literature [7–10]. Mathematical expressions for the main out of plane material properties have been presented and a parameter optimization has been carried out. A favorite multifunctional power design with a high first resonance frequency, a low material density, and a high-energy density was identified. The current study focuses on the manufacture of the optimum multifunctional power panel, introduces the experimental procedures to measure the dynamic response, and discusses the experimental results.

II. Analysis

An in depth discussion of the dynamic analysis and optimization of multifunctional power panels has been presented previously [6], and so only a short summary will be given at this point.

In the analysis, the first resonance frequency has been used as a performance index of the dynamic behavior of the 10 proposed multifunctional power structures. Raville's equation [11] for the natural frequencies of a simply supported sandwich panel was used to predict the dynamic response. This theory requires the main material properties and dimensions of the face skins and the equivalent out of plane shear modulii $G_{C_{xz,yz}}$ of the sandwich core as an input. These latter values were derived for the 10 different designs using the virtual displacement method [12]. Several deformation patterns including bending, shearing, and a combination of both were applied to model the different designs and describe their structural deformation. The presented approach incorporated different core materials and provided a simple set of equations for an effective

Received 15 March 2006; revision received 27 October 2006; accepted for publication 6 November 2006.

*Research Associate, Centre of Vibration Engineering, Mechanical Engineering.
†Senior Lecturer in Aerospace Structural Dynamics, Astronautics Research Group, School of Engineering Sciences, Highfield.
‡Principal Stress Engineer—SAMS-A, Kings Avenue.

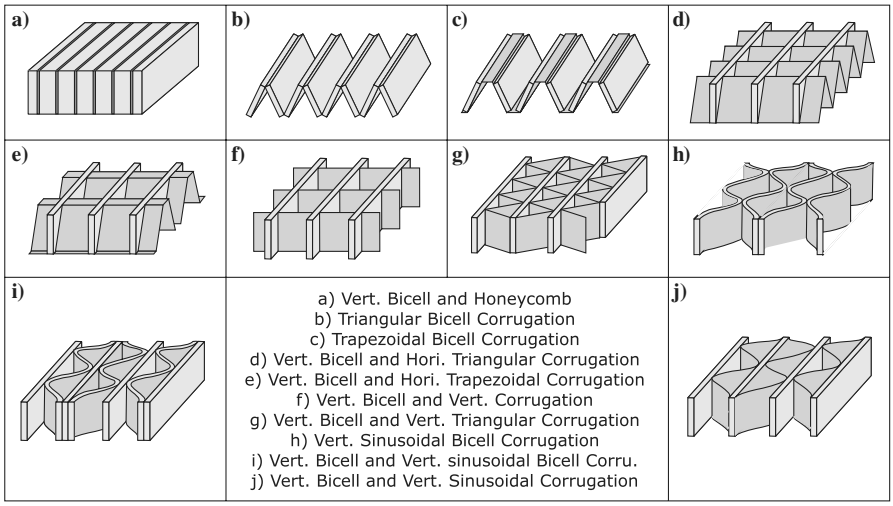

Fig. 1 The candidate multifunctional power structures.

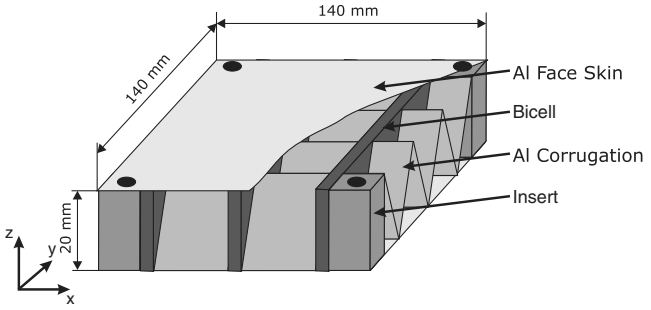

Fig. 2 Vertical bicell and horizontal triangular corrugation: concept drawing.

parameter optimization. The analytical shear properties were validated with a finite element (FE) analysis.

The 10 multifunctional power structures underwent a parameter optimization for three different sandwich panel sizes. The optimization focused on the dynamic behavior of the MFS maximizing the frequency-density ratio $\Gamma = f/\rho$ of the panels. Detailed FE models of all 10 panels validated the optimization results. The theoretical and finite element analysis led to the final manufacturing choice of a *vertical bicell and horizontal triangular corrugation* core design for the multifunctional power panel (see Fig. 2). This particular core combines flat structural batteries, which are oriented perpendicularly to the face skins, with a horizontally aligned triangular aluminum corrugation.

The batteries chosen for the multifunctional structure were Boundless Corp. structural batteries as disclosed in the literature [7–10], which provide multifunctionality at the electrode level. This makes them a primary structural element in a multifunctional sandwich panel not only providing the electrical, but also load carrying capabilities to the core. Boundless quotes an electrical capability of 0.784 W · h per cell but for the presented investigation no live batteries were available. Their main structural material properties were derived from standard shear and bending tests with an out-of-plane Young's modulus of 28 GPa and a shear modulus of 3 GPa.

III. Manufacture of the Sandwich Panels

The manufacture of the vertical bicell and horizontal triangular corrugation sandwich panel in Fig. 2 proved challenging in several respects: strongly varying geometries and different materials such as metals and composites needed to be assembled to a uniform core; the components required a high manufacturing accuracy and a good alignment to ensure a homogeneous distribution of the core material properties; and the adhesive had to ensure the integrity of the panel under static and dynamic loads. In addition to the MFS a conventional honeycomb panel with identical dimensions was built as a benchmark for the dynamic response.

a) **b)**

Fig. 3 The manufactured panels: a) MFS and b) conventional honeycomb.

A 140 mm × 140 mm × 20 mm panel with seven bicells was chosen for manufacture. The MFS panel consisted of two aluminum face skins, which were separated by the bicells and a triangular aluminum corrugation. Four aluminum inserts at each corner were added to provide an interface with the four-point support of a shaker. A face skin thickness of 1 mm and a corrugation thickness of 0.5 mm was chosen in an attempt to minimize local deformations of unsupported areas in the panel and to facilitate the manufacture of the core.

The core components (bicells, corrugations, inserts) were assembled with a two component multipurpose epoxy (Araldite) which allowed curing at room temperature. The core components were aligned inside a frame and pressure was applied from all directions to ensure a uniform geometry. In a second manufacturing step the face skins were attached to the core to complete the sandwich structure.

An additional conventional HexWeb 5.2-1/4-25(3003) aluminum honeycomb panel of the same dimensions as the MFS was also manufactured similarly to the MFS (see Fig. 3b). The corners of the honeycomb were modified to accommodate the four inserts.

IV. Four-Point Support Test Setup

The need to avoid the frequency bands most excited by launch vehicles required an experimental investigation into the dynamic response of the multifunctional sandwich panels to validate the technology. The panels were therefore mounted with a four-point support onto the shaker to capture the dynamic response from a random vibration input. Four spacers were placed between the panel and the shaker interface to separate them from each other (see Fig. 4).

Two accelerometers were placed at the axis of symmetry of two adjacent edges and a third accelerometer was located at the center of the panel. These locations allowed the capture of the first resonance response frequency and its corresponding deflection shape at resonance. The focus on the first resonance response frequency during testing was caused by the need of it for the experimental

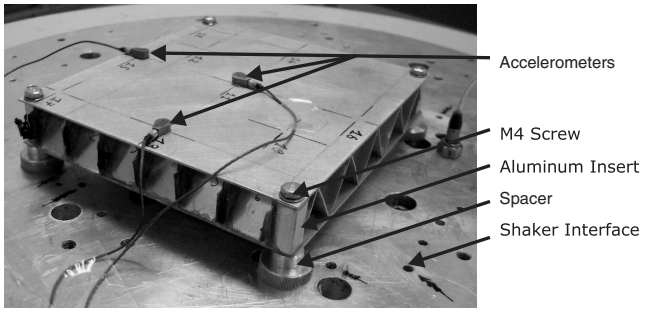

Fig. 4 The multifunctional panel on the shaker.

determination of the frequency-density ratio Γ which was used in the presented investigation to evaluate and compare the multifunctional designs. The lower frequencies also provide the strongest contribution to the introduced stresses during vibration and their accurate prediction and experimental determination is therefore most important. The panels were exposed to the random high-energy ramped spectrum in Fig. 5 with increasing energy levels ($-30, -20, -12, -9, -6, -3$ dB) up to 10 grms. A comparison of these sequential measurements allowed the detection of possible variations in the resonance response in relation to changing energy levels. The processed data allowed the determination of the dynamic response of the MFS and the honeycomb panel.

V. Detailed Finite Element Analysis

Detailed finite element models of the MFS and the conventional honeycomb sandwich panel were created in Ansys (Ver. 8) to compare the experimental results with the theoretical data. The detailed finite element model of the vertical bicell and horizontal triangular corrugation accurately represented the main features of the experimental panel. A fine mesh of 9846 SHELL63 elements was used for the core and face skins and 10,856 SOLID45 elements were used to model the inserts of the manufactured panels (see Fig. 6a). The main material properties used in the analysis are listed in Table 1.

The honeycomb core in Fig. 6b was modeled with 5592 SOLID73 elements and the face skins consisted of 1864 SHELL63 elements. The measured [13,14] main orthotropic core material properties of the HexWeb 5.2-1/4-25(3003) honeycomb core from Table 1 were used for the analysis.

Table 1 Aluminum, battery, and honeycomb material properties

	Aluminum	Battery	HexWeb 5.2-1/4-25(3003)
Young's modulus, GPa	70	28	1.03
Shear modulus xz, GPa	26.9		4.65
Shear modulus yz, GPa	26.9	3	2.51
Density, kg/m^3	2700	1785	83

The four-point support was modeled in the finite element analysis with rigid elements between the four inserts and the central shaker mass (MASS21) (see Fig. 6c). The random 10 grms spectra from Fig. 5 was applied to the shaker mass during a power spectral density (PSD) analysis to predict the first resonance response frequencies of the panels. Linear damping was assumed and the damping ratios ζ for the finite element panels were estimated by the half-power-bandwidth method from the experimental results leading to 0.82% for the MFS and 0.78% for the honeycomb panel.

VI. Effective Energy Density

The main focus of the presented experimental investigation was the determination of the dynamic response of the proposed multifunctional power structure. For the electrical properties of the panel only a theoretical investigation was carried out. The effective energy density (EED) was used to investigate the gains of this new technology [7]. It allowed a comparison with traditional energy storage devices and was defined as the energy provided by the MFS (Ene_{MFS} [W · h]) divided by the difference between the mass of the MFS (m_{MFS}) and an inert sandwich panel mass (m_{inert}) with a similar structural performance,

$$\text{EED} = \frac{\text{Ene}_{\text{MFS}}}{m_{\text{MFS}} - m_{\text{inert}}} \left[\frac{\text{W} \cdot \text{h}}{\text{kg}}\right] \tag{1}$$

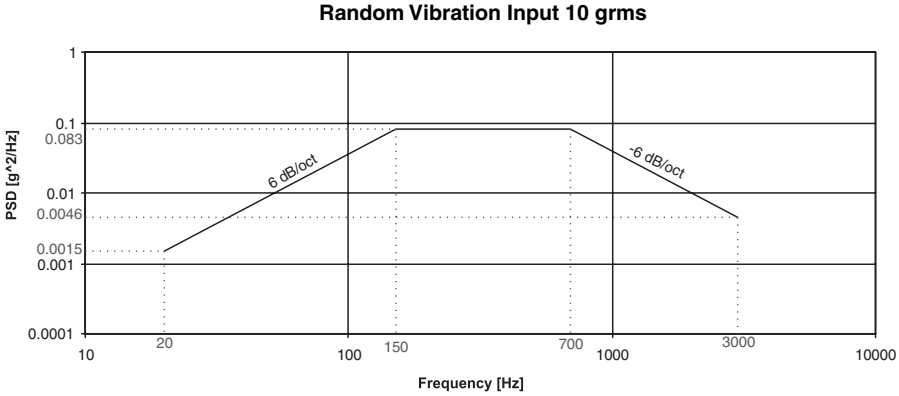

Fig. 5 The random 10 grms input spectrum.

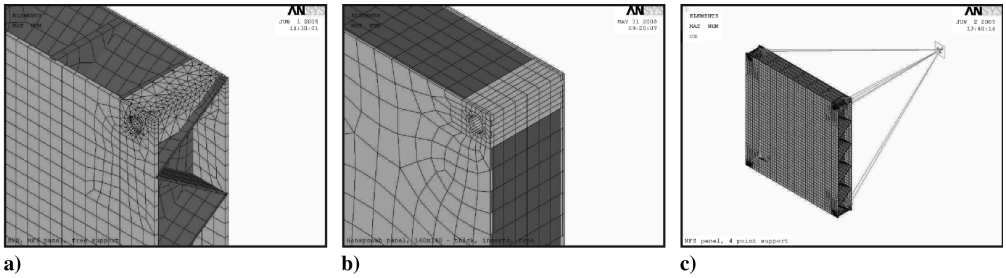

a) b) c)

Fig. 6 FE model of a) the MFS, b) the conventional honeycomb panel, and c) the four-point support.

Table 2 Energy density of traditional space batteries [15–20]

Cell chemistry	Energy density, W · h/kg
Nickel–cadmium (NiCd)	35–60
Nickel metal hydride (NiMH)	50–80
Nickel–hydrogen (NiH_2)	40–60
Lithium–ion (Li–Ion)	150–200

In theory, assuming bicells with an energy output of 0.784 W · h per cell [10], the manufactured MFS panel with seven bicells could have provided a maximum energy output of $Ene_{MFS} = 5.488$ W · h. The total mass of the manufactured MFS panel and the inert honeycomb panel was $m_{MFS} = 0.227$ kg and $m_{inert} = 0.15$ kg, respectively. This resulted in an effective energy density EED of 71.3 W · h/kg for the manufactured multifunctional power panel.

The equivalent energy density of the manufactured MFS exceeded most of the traditional energy storage systems from Table 2 but it remained below the suggested values for the recently introduced Li-Ion battery designs. An increase in the bicell output and a higher amount of batteries in the panel may provide similar levels in the future. The energy density gave a good estimation of the weight savings in a spacecraft, but it did not indicate possible volume savings of the MFS. This was considered with the volumetric effective energy density (VEED [W · h/l]) that replaced the panel mass in Eq. (1) with the panel volumes. It tended towards infinity for the presented design, as the volumes of the manufactured MFS and the comparable honeycomb panel were nearly identical, thereby far exceeding traditional systems. The volume gains using a MFS could provide space for additional payload or enable a smaller satellite structure to be built.

VII. Experimental and Finite Element Test Results

The measured dynamic response of the multifunctional power structure is shown in Figs. 7 and 8 and the corresponding first resonance response frequencies are listed in Table 3.

The MFS panel was excited up to 3000 Hz during the random vibration tests. The input autospectrum showed some control problems above 2250 Hz, but with a lower first resonance response frequency a clear determination of the dynamic response was possible. During the increase of the energy input up to 10 grms a change in the dynamic response became visible (see Fig. 7). Each higher energy level slightly decreased the resonance response frequencies and increased the damping in the structure. This behavior was a strong indication of nonlinearities in the MFS panel [21]. It could be ascribed to the known strong plastic shearing properties of the used bicells, the unknown interaction between the panel components and the adhesive, and possible inaccuracies of the manual manufacturing process. The identified first mode shape of the random vibration test was a full bending motion of the panel.

The conventional honeycomb panel in Fig. 8 had a similar dynamic behavior as the previously presented MFS panel. The random vibration showed a control problem at 2250 Hz, but with the required first resonance response frequency 25% below this value, a clear identification of the dynamic response was possible. The changes in the resonance response frequencies for different energy inputs were minimal (see Table 3) which indicated a nearly linear behavior of the honeycomb and validated the chosen manufacturing process for the panels.

The dynamic response of the finite element models is shown in Fig. 9. The four-point support led to a first bending mode of the panels with a maximum deformation in the center. A very regular overall deformation was predicted with no significant local deformations of the unsupported face skin areas.

VIII. Discussion

The MFS and the conventional honeycomb panel provided good experimental results during vibration testing. A satisfactory energy input and excitation of the investigated frequency range was achieved. The MFS and the honeycomb panel showed a comparable dynamic behavior. The location of the accelerometers at the intersection of the bicells and the corrugation allowed a clear identification of the resonance response frequencies and the corresponding deflection shapes.

The experiments revealed a nonlinear behavior of the vertical bicell and horizontal triangular corrugation panel which was not detectable in the honeycomb panel response. This nonlinear behavior was ascribed to the bicell and the adhesive material properties and the different layouts of the panels. The frequency variations for the MFS and honeycomb panels caused by the nonlinearities were less than 1.5 and 0.3%, respectively, in Table 3, indicating the rather small influence of this behavior on the two panels. The MFS panel had up

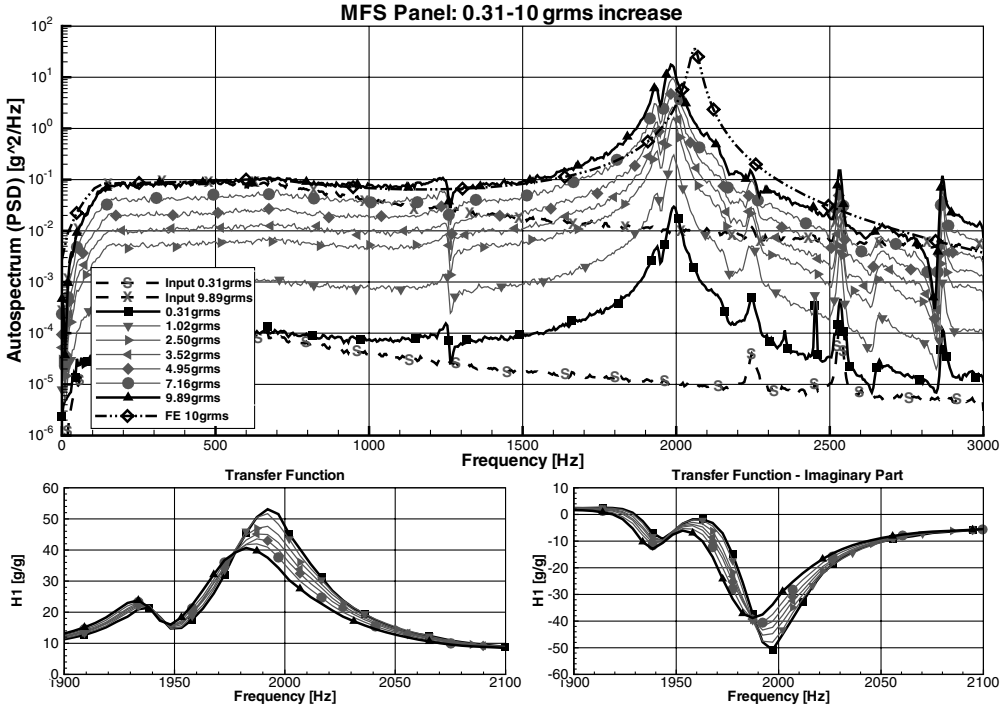

Fig. 7 MFS panel: experimental response and FE prediction.

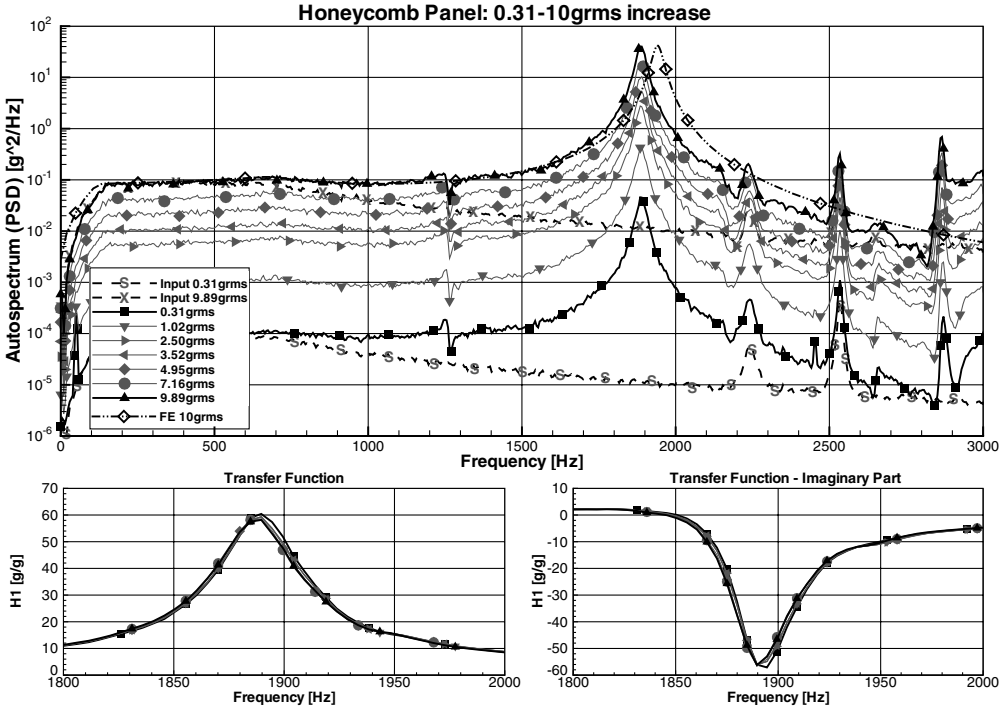

Fig. 8 Honeycomb panel: experimental response and FE prediction.

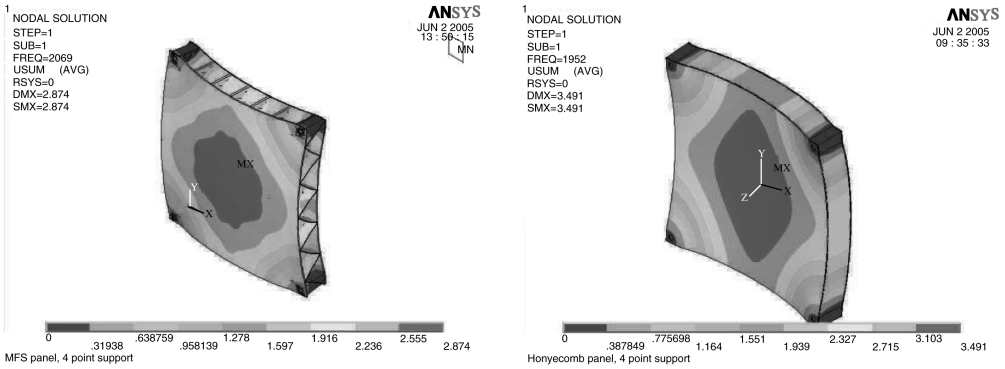

Fig. 9 FE model: first mode shape of the MFS and honeycomb panel.

to 5% higher resonance response frequencies than the honeycomb panel.

For a final evaluation of the manufactured panels the experimental dynamic response and the finite element analysis are summarized in Table 4. The MFS and the honeycomb panel showed a good agreement between the experimental and finite element results with a variation of only 2–3% for the frequency-density ratio Γ as the main performance index. The resonance frequencies of the finite element models were slightly higher than the measured values. This highlighted the influence of the perfect geometry and the linear damping of the FE models. The slightly higher densities of the finite element MFS panel were related to the averaged dimensions of the core components for the finite element panels and possible geometrical inaccuracies of the manufactured panels.

The optimized vertical bicell and horizontal triangular corrugation design fulfilled its set expectations and provided a comparable dynamic response to a conventional honeycomb panel. This strongly suggested its applicability for future lightweight, cost efficient spacecraft.

Table 3 The first resonance response frequencies for the panels

	MFS panel	Honeycomb panel
4-point: shaker—0.31–10 grms (Hz)	1992–1984	1888–1888
4-point: finite element (Hz)	2069	1952

Table 4 Comparison of the measurement and finite element results

	MFS		Honeycomb	
	Test	FE	Test	FE
Γ ratio, Hz $\cdot$ m^3/kg	3.68	3.75	5.26	5.43
Frequency, Hz	1984	2069	1888	1952
Density, kg/m^3	539	551	359	359

IX. Conclusion

In this paper, the manufacture of a multifunctional vertical bicell and horizontal triangular corrugation sandwich panel has been described. The dynamic behavior of the MFS has been determined experimentally. Detailed finite element models of the manufactured panels completed the investigation.

A similar dynamic response of the optimized multifunctional power structure and the conventional honeycomb panel was detected, which successfully proved the reliability of the vertical bicell and horizontal triangular corrugation concept. A good agreement between the experimental data and the finite element results was found.

The multifunctional power structure fulfilled all its set expectations, providing a similar dynamic behavior to conventional

honeycomb structures with the additional functionality of a secondary power storage. The effective energy density of the MFS panel exceeded current traditional battery systems and provided significant volume gains. This made it an excellent design approach for future space missions.

References

[1] Jilla, C. D., and Miller, D. W., "Satellite Design: Past, Present and Future," *International Journal of Small Satellite Engineering*, No. 1 [online journal], Centre for Satellite Engineering Research, Guildford, Surrey, U.K., http://www.ee.surrey.ac.uk/SSC/CSER/UOSAT/IJSSE/issue1/cjilla/cjilla.html [retrieved 24 Nov. 2005].

[2] Haake, J. M., Jacobs, J. H., and McIlroy, B. E., "Thick Walled Carbon Composite Multifunctional Structures,"*Proceedings of the SPIE International Society for Optical Engineering*, Vol. 3041, 1997, pp. 32–43.

[3] Rossoni, P., and Panetta, P. V., "Developments in Nano-Satellite Structural Subsystem Design at NASA-GSFC," SCC Paper 99-V3, 1999.

[4] Das, A., and Obal, M. W., "Revolutionary Satellite Structural Systems Technology: A Vision for the Future," *Proceedings of 1998 IEEE Aerospace Conference*, IEEE, Piscataway, NJ, 1998, Vol. 2, pp. 57–67.

[5] Snelling, M., Hobbs, S., Bowling, T., Kirby, P., Gabriel, S., Sandford, M., and Lawes, R., "AMSTAP—A UK Partnership to Develop and Apply Microsystem Technology in Space," *3rd Round Table on Micro/Nano-Technologies for Space*, ESA-ESTEC, Noordwyk, 2000.

[6] Schwingshackl, C. W., Aglietti, G. S., and Cunningham, P. R., "Parameter Optimisation of the Dynamic Behaviour of Inhomogeneous Multifunctional Power Structures," *AIAA Journal*, Vol. 44, No. 10, 2006, pp. 2286–2294.

[7] Lyman, P. C., and Feaver, T. L., "Powercore Combining Structure and Batteries for Increased Energy to Weight Ratio," *IEEE Aerospace and Electronic Systems Magazine*, Vol. 13, No. 9, 1998, pp. 39–42.

[8] Metzger, W., Westfall, R., Hermann, A., and Lyman, P., "Nickel Foam Substrate for Nickel Metal Hydride Electrodes and Lightweight Honeycomb Structures," *International Journal of Hydrogen Energy*, Vol. 23, No. 11, 1998, pp. 1025–1029.

[9] Olson, J. B., Feaver, T. L., and Lyman, P. C., "Structural Lithium-Ion Batteries Using Dual-Functional Carbon Fabric Composite Anodes," *Proceedings of the 14th International Conference on Composite Materials*, SME, Dearborn, July 2003.

[10] Olson, J., Shaw, Z., Jennings, J., Lyman, V., Feaver, T., and Lyman, P., "Structural High Power Energy Storage Panels Using Dual-Functional Carbon Fabric Composite Electrodes," *Space Power Workshop*, Aerospace Corp., El Segundo, 2003.

[11] Raville, M. E., and Ueng., C. E. S., "Determination of Natural Frequencies of Vibration of a Sandwich Plate," *Experimental Mechanics*, Vol. 7, No. 11, 1967, pp. 490–493.

[12] Parkus, H., *Mechanik der festen Körper*, 2nd ed., Springer–Verlag, Wien, 1995.

[13] "C365 Standard Test Methods for Flatwise Compressive Strength of Sandwich Cores," American Society for Testing and Materials, 1988.

[14] "C273 Standard Method of Shear Test in Flatwise Plane of Flat Sandwich Constructions or Sandwich Cores," American Society for Testing and Materials, 1970.

[15] Hill, C. A., "Satellite Battery Technology—A Tutorial and Overview," *Proceedings of 1998 Institute of Electrical and Electronic Engineers (IEEE) Aerospace Conference*, IEEE, New York, 1998, Vol. 1, pp. 153–158.

[16] Teofilo, V. L., Isaacson, M. J., Higgins, R. L., and Cuellar, E. A., "Advanced Lithium Ion Solid Polymer Electrolyte Battery Development," *IEEE Aerospace and Electronic Systems Magazine*, Vol. 14, No. 11, 1999, pp. 43–47.

[17] Teofilo, V. L., and Nadell, J. N., "Aerospace Lithium Solid Polymer Batteries," *IEEE Aerospace and Electronic Systems Magazine*, Vol. 13, No. 5, 1998, pp. 33–36.

[18] Fortescue, P., and Stark, J., *Spacecraft Systems Engineering*, 2nd ed., Wiley, Chichester, 1995.

[19] Vincent, C. A., and Scrosati, B., *Modern Batteries: An Introduction to Electrochemical Power Sources*, 2nd ed., Butterworth–Heinemann, Oxford, 2003.

[20] Cole, J. H., Eskra, M., and Klein, M., "Bipolar Nickel-Metal Hydride Batteries for Aerospace Applications," *IEEE Aerospace and Electronic Systems Magazine*, Vol. 15, No. 1, 2000, pp. 39–45.

[21] Ewins, D. J., *Modal Testing: Theory, Practice and Application*, 2nd ed., Research Studies Press LTD, Letchworth, 2000.

A. Roy
Associate Editor